Proceeding Paper

Assessing the Strategic Preparation of Coordination Polymer Particles: A Computational Analysis of the Impact of Different Catechol-Based Ligands †

Matías Capurso [ID], Gabriel Radivoy [ID], Fabiana Nador [ID] and Viviana Dorn *[ID]

Instituto de Química del Sur (INQUISUR-CONICET), Departamento de Química, Universidad Nacional del Sur, Av. Alem 1253, Bahía Blanca B8000CPB, Argentina; matias.capurso@uns.edu.ar (M.C.); gradivoy@criba.edu.ar (G.R.); fabiana.nador@uns.edu.ar (F.N.)

* Correspondence: vdorn@uns.edu.ar

† Presented at the 27th International Electronic Conference on Synthetic Organic Chemistry (ECSOC-27), 15–30 November 2023; Available online: https://ecsoc-27.sciforum.net/.

Abstract: DFT calculations were applied to an iron/catechol derivative system to investigate their effect on the structure of CPPs as a function of (a) metal valence—Fe^{+2} and Fe^{+3} in high- and low-spin states; (b) type of chelating groups in the catechol derivatives and their geometries; and (c) the aliphatic chain length between two chelating groups in a model polydentate ligand. The results indicate that catechol-pyridine and bis-catechol ligands, with Fe^{+3} salts, are promising combinations to synthesize CPPs. In addition, the inclusion of an aliphatic chain with four carbons between the chelating groups could enhance polymerization versus monomer formation.

Keywords: CPPs; catechol; DFT

1. Introduction

Catechol derivatives are promising for use as functional materials [1] due to their metal-chelating ability [2], making them excellent ligands for generating Coordination Polymer Particles (CPPs). They self-assemble into CPPs from metal ions and polydentate organic ligands (Figure 1) [3]. Up until now, polymeric structure characterization remains challenging; however, being able to predict CPP properties such as morphology, size and stability in diverse environments is essential for their applications.
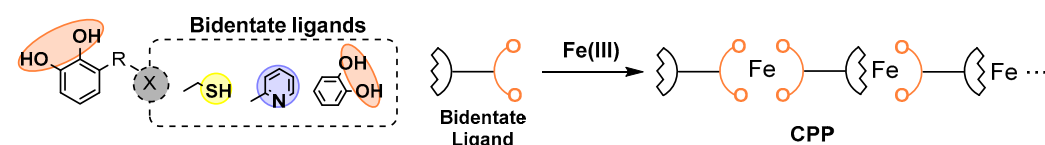

Figure 1. Formation of CPPs.

In this study, we present findings from conducting DFT calculations on iron/catechol derivative systems, with the primary functional groups being considered for use in CPP synthesis (Figure 1). We then conducted an analysis of the results to better understand their impact on the CPP synthesis process.

2. Methods

All computations in this work were carried out with the ORCA 5.0 program package [4,5]. Geometry optimizations of the high-spin and low-spin states for each complex were performed with the BP86 density functional [6] with D3BJ dispersion correction [7,8], a methodology widely used for this type of complex [9]. Single-point energy calculations were carried out with wB97X [10] with D3BJ dispersion correction. The def2 TZVPP (Fe),

TZVP (O, N, S) and SVP (other) basis sets [11] were applied in the geometry optimizations and single-point calculations.

3. Results and Discussion

The synthesis and properties of CPPs are highly dependent on the type of metal ion used, the chelating groups present in the ligands and their structure. In this context, by employing DFT calculations on an iron/catechol derivative system, we investigated the effect on the structure of CPPs based on:

- The use of Fe^{+3} and Fe^{+2} in high- and low-spin states;
- The type of chelating groups in catechol derivatives as well as their geometries;
- The aliphatic chain length between the two chelating groups in a model polydentate ligand.

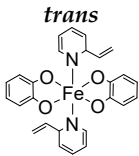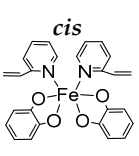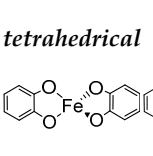#### *3.1. Analysis of Metallic Species and Organic Chelating Groups*
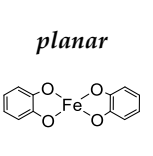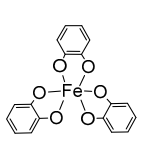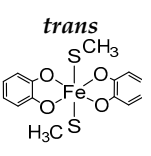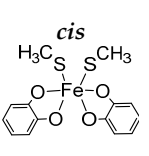
As previously mentioned, the formation of iron complexes with simplified representative structures of the ligands and the Fe^{+2} and Fe^{+3} species in high- and low-spin states were considered. It is known that other Fe^{+3} complexes with catechol derivatives exhibit high-spin ferric species [12,13], and we found the same trend—all the high-spin Fe^{+3} complexes were approximately 20 kcal/mol energetically more stable than that their low-spin counterparts (Table 1). A comparable trend was observed for Fe^{+2} complexes.

Table 1. High/low spin energy differences (kcal/mol) for the iron complexes.

Complex	Fe^{+3}	Fe^{+2}
trans-Fe(cat)$_2$(pyr)$_2$	−12	−21
cis-Fe(cat)$_2$(pyr)$_2$	−22	−18
Fe(cat)$_2$	−21	−25
Fe(cat)$_3$	−28	−45
trans-Fe(cat)$_2$(thiol)$_2$	−21	−34
cis-Fe(cat)$_2$(thiol)$_2$	−24	−57

In a subsequent step, the binding energies for the high-spin iron complexes were evaluated and the results are compared in Table 2. According to the results, Fe^{+3} complexes were more stable than Fe^{+2} complexes, with binding energies approximately twice as high. As can be seen from Table 2, for the *trans*-Fe[(cat)$_2$(pyr)$_2$] complexes, the Fe^{+3} complex, has a binding energy of 1609 kcal/mol, whereas the Fe^{+2} analog has a binding energy of 848 kcal/mol.

Table 2. Binding energy of high-spin iron complexes (kcal/mol).

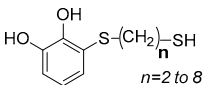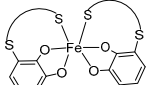| Metallic ion	[Fe(cat)$_2$(pyr)$_2$]		[Fe(cat)$_2$]		[Fe(cat)$_3$]	[Fe(cat)$_2$(thiol)$_2$]	
	trans	*cis*	*tetrahedrical*	*planar*		*trans*	*cis*
Fe^{+3}	−1609	−1602	−1582	−1569	−1558	−1455	−1460
Fe^{+2}	−848	−838	−832	−831	−648	−546	−570
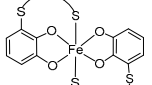
Considering the binding energy of high-spin Fe^{+3} complexes, it was observed that those with catechol-pyridine as ligands were more stable, favoring the *trans* geometry (1609 kcal/mol) over the *cis* (1602 kcal/mol) by 7 kcal/mol. Fe(cat)$_2$ and Fe(cat)$_3$ complexes followed them in stability, whereas catechol–thiol complexes proved to be the least stable, as can be seen in Table 2. The same trend was observed for Fe^{+2} complexes.

Based on these results, we could assume that the use of Fe(III) salts in combination with catechol-pyridine or bis-catechol ligands appears to be the most appropriate combination for the synthesis of CPPs.

3.2. Effect of the Methylene Spacers between the Chelating Groups

To examine the influence of the aliphatic chain length between the two chelating groups, a ligand model of 3-((5-mercapto*alkyl*)thio)benzene-1,2-diol was used, with the alkyl chain ranging from two to eight methylene groups (Table 3). The length and conformation of this alkylic chain could significantly affect the formation of the CPPs, as it may precipitate as a stable monomer, thereby inhibiting polymer growth.
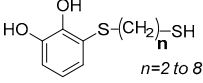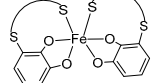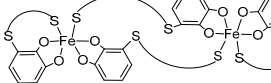
Table 3. Structure of the ligand model and relative binding energies of the *cis* and *trans* monomers.

model ligand n =	cis-monomer (kcal/mol)	trans-monomer (kcal/mol)	$\Delta E = E_{cis} - E_{trans}$ (kcal/mol)
2	no formation	no formation	-
3	0	5	−5
4	16	21	−5
6	29	34	−6
8	46	50	−4

We calculated the formation of the possible *cis* and *trans* isomers of the monomers between high-spin Fe^{+3} and the model ligand. As can be observed from Table 3, to obtain both, *cis*- and *trans*-monomers, at least three methylene groups were necessary as alkyl spacers in the alkyl chain. Additionally, the *cis* complexes were approximately 5 kcal/mol more stable than the *trans* complexes. It is also observed that as the methylene spacer decreases in length, the monomers increase their stability. For the *cis* isomer, Table 3 shows an energy stabilization of 46 kcal/mol when methylene groups reduce from eight to three, and 50 kcal/mol for the *trans* isomer.

The same analysis was carried out to examine dimer formation, and their relative energy values are presented in Table 4. It was found that dimer formation was more favorable with four methylene groups in the alkyl chain. On the other hand, isolated monomers appeared to be more energetically stable compared to the dimers; however, as the length alkylic chain increased, the formation of the dimers became progressively more favorable.

Table 4. Structure of the ligand model and relative binding energies of cis monomer and dimer.

model ligand n=	cis-monomer (kcal/mol)	dimer (kcal/mol)	$\Delta E = E_{dim} - E_{mon}$ (kcal/mol)
3	0	11	11
4	16	0	−16
6	29	20	−8
8	46	39	−6

According to the obtained results, we can assume that the incorporation of an alkyl spacer of at least four methylene groups between the chelating groups could be more advantageous for polymer formation over monomer formation, thus favoring the synthesis of the CPPs.

The structures are currently being recalculated by incorporating solvent and other metal ions, both of which are factors that can affect the energy and/or structure of the CPPs.

4. Conclusions

DFT calculations are a powerful tool for investigating the structure and properties of CPPs. Based on these findings, catechol-pyridine and bis-catechol ligands, with Fe^{+3} as the metallic ion, would form structures potentially suitable for synthesizing CPPs.

The analysis on the effect of the methylene spacers between the chelating groups could indicate that a shorter spacer of at least three methylenes promotes monomer formation, while increasing the spacer to four or more methylenes improves the possibility of polymerization.

Future research is focused on the impact of additional factors on the structure of CPPs, such as the presence of solvent molecules and other metallic ions.

Author Contributions: V.D. carried out the conceptualization, investigation, methodology and writing; F.N. participated in the investigation, methodology and writing; M.C. participated in the methodology; G.R. carried out the funding acquisition, project administration, investigation and writing. All authors have read and agreed to the published version of the manuscript.

Institutional Review Board Statement: Not applicable.

Informed Consent Statement: Not applicable.

Data Availability Statement: Data available upon request.

Conflicts of Interest: The authors declare no conflict of interest.

References

1. Zhang, W.; Wang, R.; Sun, Z.; Zhu, X.; Zhao, Q.; Zhang, T.; Cholewinski, A.; Yang, F.; Zhao, B.; Pinnaratip, R.; et al. Catechol-Functionalized Hydrogels: Biomimetic Design, Adhesion Mechanism, and Biomedical Applications. *Chem. Soc. Rev.* **2020**, *49*, 433–464. [CrossRef] [PubMed]
2. Saiz-Poseu, J.; Mancebo-Aracil, J.; Nador, F.; Busqué, F.; Ruiz-Molina, D. The Chemistry behind Catechol-Based Adhesion. *Angew. Chem. Int. Ed.* **2019**, *58*, 696–714. [CrossRef] [PubMed]
3. Suárez-García, S.; Solórzano, R.; Novio, F.; Alibés, R.; Busqué, F.; Ruiz-Molina, D. Coordination Polymers Nanoparticles for Bioimaging. *Coord. Chem. Rev.* **2021**, *432*, 213716. [CrossRef]
4. Neese, F. The ORCA Program System. *WIREs Comput. Mol. Sci.* **2012**, *2*, 73–78. [CrossRef]
5. Neese, F. Software Update: The ORCA Program System—Version 5.0. *WIREs Comput. Mol. Sci.* **2022**, *12*, e1606. [CrossRef]
6. Perdew, J.P. Density-Functional Approximation for the Correlation Energy of the Inhomogeneous Electron Gas. *Phys. Rev. B* **1986**, *33*, 8822–8824. [CrossRef] [PubMed]
7. Grimme, S.; Antony, J.; Ehrlich, S.; Krieg, H. A Consistent and Accurate Ab Initio Parametrization of Density Functional Dispersion Correction (DFT-D) for the 94 Elements H-Pu. *J. Chem. Phys.* **2010**, *132*, 154104. [CrossRef] [PubMed]
8. Grimme, S.; Ehrlich, S.; Goerigk, L. Effect of the Damping Function in Dispersion Corrected Density Functional Theory. *J. Comput. Chem.* **2011**, *32*, 1456–1465. [CrossRef] [PubMed]
9. Neese, F. A Critical Evaluation of DFT, Including Time-Dependent DFT, Applied to Bioinorganic Chemistry. *J. Biol. Inorg. Chem.* **2006**, *11*, 702–711. [CrossRef] [PubMed]
10. Chai, J.-D.; Head-Gordon, M. Long-Range Corrected Hybrid Density Functionals with Damped Atom–Atom Dispersion Corrections. *Phys. Chem. Chem. Phys.* **2008**, *10*, 6615. [CrossRef] [PubMed]
11. Weigend, F.; Ahlrichs, R. Balanced Basis Sets of Split Valence, Triple Zeta Valence and Quadruple Zeta Valence Quality for H to Rn: Design and Assessment of Accuracy. *Phys. Chem. Chem. Phys.* **2005**, *7*, 3297. [CrossRef]

12. Orville, A.M.; Lipscomb, J.D. Binding of Isotopically Labeled Substrates, Inhibitors, and Cyanide by Protocatechuate 3,4-Dioxygenase. *J. Biol. Chem.* **1989**, *264*, 8791–8801. [CrossRef]
13. Whittaker, J.W.; Lipscomb, J.D.; Kent, T.A.; Münck, E. Brevibacterium Fuscum Protocatechuate 3,4-Dioxygenase. Purification, Crystallization, and Characterization. *J. Biol. Chem.* **1984**, *259*, 4466–4475. [CrossRef] [PubMed]